


## Using Pulsar Parameter Drifts to Detect Subnanohertz Gravitational Waves

William DeRocco<sup>1</sup> and Jeff A. Dror<sup>2</sup>

*Department of Physics, University of California Santa Cruz, 1156 High Street, Santa Cruz, California 95064, USA  
and Santa Cruz Institute for Particle Physics, 1156 High Street, Santa Cruz, California 95064, USA*

 (Received 27 February 2023; revised 25 August 2023; accepted 17 January 2024; published 8 March 2024)

Gravitational waves with frequencies below 1 nHz are notoriously difficult to detect. With periods exceeding current experimental lifetimes, they induce slow drifts in observables rather than periodic correlations. Observables with well-known intrinsic contributions provide a means to probe this regime. In this Letter, we demonstrate the viability of using observed pulsar timing parameters to discover such “ultralow” frequency gravitational waves, presenting two complementary observables for which the systematic shift induced by ultralow-frequency gravitational waves can be extracted. Using existing data for these parameters, we search the ultralow-frequency regime for continuous-wave signals, finding a sensitivity near the expected prediction from inspirals of supermassive black holes. We do not see an excess in the data, setting a limit on the strain of  $1.3 \times 10^{-12}$  at 450 pHz with a sensitivity dropping approximately quadratically with frequency until 10 pHz. Our search method opens a new frequency range for gravitational wave detection and has profound implications for astrophysics, cosmology, and particle physics.

DOI: [10.1103/PhysRevLett.132.101403](https://doi.org/10.1103/PhysRevLett.132.101403)

**Introduction.**—In the era of gravitational wave (GW) astronomy, extending our observational capacity over the frequency spectrum has become a top priority. Existing experiments cover a large range of frequencies; tests for cosmic microwave background tensor modes [1] probe the  $10^{-18}$  Hz to  $10^{-16}$  Hz range, existing pulsar timing array (PTA) analyses search the 1 nHz to 100 nHz range [2–5], and laser interferometers are already detecting GWs in the 10 Hz to 1 kHz range [6]. Future space-based interferometers, such as the Laser Interferometer Space Antenna, will cover 1 mHz to 1 Hz [7], while underground experiments [8,9] aim to target the region between ground-based and space-based interferometry. There has been significant discussion on potential observational techniques in the  $\mu$ Hz to mHz range [10–19] and above the kHz range [20–22] to expand our GW frequency coverage.

Despite these efforts, a significant gap in our experimental efforts remains in the spectrum between cosmic microwave background polarization and PTA analyses,  $10^{-16}$  Hz to  $10^{-9}$  Hz. This “ultralow frequency” range is strongly motivated by the expectation of GWs from supermassive black hole (SMBH) binary inspirals [23,24] (see also Refs. [25–28] for examples of possible cosmic sources).

The detection of ultralow-frequency GWs is a significant experimental challenge since their period exceeds experimental timescales (e.g., up to thirty years for existing PTAs). In the context of PTAs, the effect of GWs at these low frequencies is to induce secular drifts in pulse arrival times instead of oscillatory features. Traditional pulsar timing searches fit a set of timing model parameters to the times of arrival, then subtract away this fit to search for

correlations in the residuals (while simultaneously marginalizing over small deviations in the fit parameters). In this paper, we demonstrate that rather than searching for signal in the residuals, one can instead perform a search using the measured values of the fit parameters themselves. This provides a powerful alternative analysis strategy for the detection of ultralow-frequency GWs. While our analysis relies on polynomial approximations of a GW signal, hence cannot reach the sensitivity of a dedicated search using the pulse times of arrival, our analysis is intuitive, computationally-efficient, and provides an easy means of extending a search to ultralow frequencies.

We perform a search using existing data for two complementary timing model parameters: the second derivative of the pulsar period with respect to time and the orbital decay of pulsars in binary systems. Our work builds on existing literature [29–38] in multiple key ways [39]. Firstly, we use an array of pulsars to search for GWs rather than a single, well-measured pulsar, as cross-sky correlations provide a critical method to discriminate over noise sources. Secondly, we simultaneously use information from binary pulsar orbital parameters and single pulsar parameters. As we will show, these observables are sensitive to different powers of signal frequency; detecting a signal with both methods gives critical information about the source. Finally, we apply our strategy to existing data to search for signatures of continuous GWs sourced by individual SMBH binaries. While we do not find significant evidence for GWs in our data, the results reach sensitivities to GWs within the expected range for these sources.

**Gravitational waves in PTAs.**—Influence on pulsar timing: Pulsar timing array experiments measure periodic

radio emissions from millisecond pulsars over timescales of decades, with data taken for each pulsar approximately once every few weeks and observed for around 1 h. The pulses in each observation period are folded together to produce a single time of arrival (TOA) associated with that observation, denoted  $t_{\text{obs}}^i$  for observation  $i$ .

Existing PTA analyses proceed as follows: the observed TOAs  $\{t_{\text{obs}}^i\}$  for a given pulsar are fit to a timing model  $\bar{t}(\lambda)$ , where we use  $\lambda$  to denote the set of model parameters. We assume the timing model is extensive, meaning it has sufficient parameters to encapsulate all secular drifts. (We elaborate on the influence of truncating the timing model to a nonextensive parameter set in the ‘‘GWs as secular drifts’’ section below.) The output of the fitting procedure is a set of best-fit parameters  $\hat{\lambda}$ , such that the difference between the observed TOAs and expected TOAs is minimized. These differences are the ‘‘timing residuals,’’  $t_{\text{obs}}^i - \bar{t}^i(\hat{\lambda})$ . The periodic oscillations of GWs with frequencies above the inverse time span of the experiment,  $f_{\text{GW}} \gtrsim T^{-1} \simeq 1$  nHz, induce oscillatory correlations in these timing residuals. These correlations are the target of all traditional PTA analyses.

GWs with frequencies below the inverse time span of the experiment,  $f_{\text{GW}} \lesssim T^{-1}$ , manifest as low-frequency changes in the TOAs, also known as ‘‘secular drifts.’’ If the pulsar timing model is extensive, ultralow-frequency GWs are removed from the residuals by the fitting procedure. Nevertheless, one can still search for GWs through the induced biases in the best-fit parameters.

The list of model parameters used is pulsar-specific [44], though it includes the pulsar period ( $P$ ), its rate of change ( $\dot{P}$ ), and potentially higher derivatives. If the pulsar is in a binary, the timing model will additionally include the binary period ( $P_b$ ) and its derivative ( $\dot{P}_b$ ). The observed values of these parameters are modified in the presence of ultralow-frequency GWs. Their dominant effect can be described through an apparent relative motion between the solar system barycenter (SSB) and the pulsar. We write this effect in terms of a relative velocity (more commonly known as redshift in the literature),

$$v_{\text{GW}}(t) = \sum_{A=+, \times} F_A(\hat{n})(h_A(t, 0) - h_A(t - d_a, \mathbf{d}_a)), \quad (1)$$

where the subscript  $A = +, \times$  denotes the cross or plus polarization of the wave, and we use  $\mathbf{d}_a$  to denote a displacement vector from the SSB to pulsar- $a$  in a frame with the SSB at the origin. We work in units such that the speed of light is set to unity. The  $h_{+, \times}(t, \mathbf{x})$  functions describe a periodic GW source at position  $\mathbf{x}$ . The quadrupolar nature of the wave imprints a particular pattern of contraction or expansion, captured in the ‘‘pattern functions,’’

$$F_A(\hat{n}) \equiv \frac{\hat{d}_a^i \hat{d}_a^j \hat{e}_{ij}^A(\hat{n})}{2(1 + \hat{n} \cdot \hat{d}_a)}, \quad (2)$$

where  $\hat{e}_{ij}$  are the polarization tensors and  $\hat{n}$  is the unit vector pointing toward the source. We provide a derivation of Eq. (1) to clarify its identification as a velocity in the Supplemental Material (SM) [45], following Ref. [61].

Because of the strong astrophysical motivation in this frequency band, we search for a signal from an individual SMBH binary. The form of  $h_A(t, \mathbf{x})$  for this source is well-known and is given approximately as a sinusoid with frequency  $f_{\text{GW}}$  and amplitude set by the dimensionless strain  $h_0$  [62]. The full form and a discussion of the associated orbital parameters are presented in the SM [45].

GWs as secular drifts: The fitting procedure captures induced accelerations and jerks as systematic shifts in the observed parameter values; we explicitly include the subscript ‘‘obs’’ to remind the reader that the best-fit parameters are *not* equal to the true physical parameters. For the pulsar period ( $P$ ) and binary period ( $P_b$ ), the observed values are close to the fundamental values, and we do not include this subscript on their symbols. The observed parameters contain known contributions that can be generically broken into three main classes: (1) *intrinsic* contributions, which are due to physical effects within the pulsar system such as electromagnetic or gravitational radiation liberating energy from the system; (2) *observational* contributions, which are effects induced due to relative motion between the SSB and pulsar, and (3) *galactic* contributions, which are induced by the Milky Way (MW) potential.

The timing model parameters can also be biased if pulsars have an unknown wide binary companion, are in a globular cluster, or carry mischaracterized ultralow-frequency red noise. We search for such effects in the SM [45].

We now consider the known contributions to the pulsar timing model parameters for models of millisecond pulsars, starting with the observed pulsar spin-down rate,

$$\frac{\dot{P}_{\text{obs}}}{P} = \frac{\dot{P}_{\text{int}}}{P} - \frac{v_{\perp}^2}{d_a} - a_{\text{MW}} - a_{\text{GW}}. \quad (3)$$

The first contribution on the right-hand side is the intrinsic spin-down of the pulsar due to electromagnetic radiation. The second term is a kinematic term arising from the motion of the pulsar (the ‘‘Shklovskii effect’’ [63]) proportional to the relative motion of the pulsar perpendicular to the line of sight ( $v_{\perp}$ ). The third term is a relative acceleration induced by the Milky Way potential. The fourth term is a relative acceleration induced by a passing GW [which we aim to observe and can be calculated from Eq. (1)].

While the effect of GWs is contained within  $\dot{P}_{\text{obs}}$ , it is necessary to subtract off the intrinsic, kinematic, and galactic contributions to  $\dot{P}_{\text{obs}}$  to extract it. Despite the observed value of this parameter being precisely measured (typical uncertainties on  $\dot{P}_{\text{obs}}/P$  reach  $10^{-24} \text{ sec}^{-1}$ ), extracting the GW contribution is not feasible due to the

inherent uncertainty in the intrinsic spin-down contribution. Predicting  $\dot{P}_{\text{int}}$  of a millisecond pulsar, whose value is of order  $1 \times 10^6$  times larger than the uncertainty on  $\dot{P}_{\text{obs}}$ , requires modeling the complex magnetic structure surrounding the pulsar, a procedure subject to large systematic uncertainties. These uncertainties make any extraction of a GW signal on a pulsar-by-pulsar basis impossible. Since GWs have a characteristic pattern across the sky that is uncorrelated with  $\dot{P}_{\text{int}}$ , GWs can still be extracted from  $\dot{P}_{\text{obs}}$  statistically, as proposed and studied in Refs. [35–38].

Statistical measurements of GWs using  $\dot{P}$  are limited since we have precise measurements of approximately 100 stable millisecond pulsars. A more sensitive approach is to consider model parameters with relatively small known contributions that can be precisely estimated. Two such parameters are the derivative of the binary period  $\dot{P}_b$  and the second derivative of the pulsar spin period  $\ddot{P}$ . The contributions to their observed values are

$$\frac{\dot{P}_{b,\text{obs}}}{P_b} = \frac{\dot{P}_{b,\text{int}}}{P_b} - \frac{v_{\perp}^2}{d_a} - a_{\text{MW}} - a_{\text{GW}}, \quad (4)$$

$$\frac{\ddot{P}_{\text{obs}}}{P} = j_{\text{GW}}. \quad (5)$$

Equation (4) is identical in structure to Eq. (3), but the intrinsic contribution is now driven by gravitational radiation emitted by the binary system. Measurements of  $\dot{P}_{b,\text{obs}}/P_b$  can reach uncertainties similar to those on  $\dot{P}_{\text{obs}}/P$  but have a critical difference: the value of  $\dot{P}_{b,\text{int}}/P_b$  is predictable once the properties of the binary components are determined. The dominant uncertainty in isolating Eq. (4) for a passing GW for many of the most sensitive pulsars is in estimating the Shklovskii term. This requires an independent measurement of  $v_{\perp}$  and  $d_a$  and can be achieved through very-long-baseline interferometry, astrometry, and pulsar timing. The Milky Way potential is typically an insignificant contribution to Eq. (4), though it can be modeled. With all these contributions estimated, we can extract GW-induced acceleration.

In the case of  $\ddot{P}$ , there are a set of corrections analogous to those in Eq. (4). However, the current uncertainty on  $\ddot{P}_{\text{obs}}$  is too large to detect their values for old millisecond pulsars. Models of magnetic dipole braking suggest the intrinsic contribution to Eq. (5) should be of order  $(\dot{P}/P)^2$  [64], which is typically on the order of  $10^{-35} \text{ sec}^{-2}$ , much below typical uncertainties on the observed value and below the gravitational wave strength we wish to target. Furthermore, since kinematic and galactic contributions to  $\ddot{P}_{\text{obs}}$  are suppressed due to the nonrelativistic nature of the galaxy, they can be neglected. We calculate the form of corrections to Eq. (5) and estimate their size in the SM [45] using the formalism presented in Ref. [65].

The sensitivity of PTA analyses to ultralow-frequency GWs is not limited to the timing model parameters presented here. Firstly, one could consider higher-order derivatives of  $P$  or  $P_b$ . Similar to  $\dot{P}$ , these will have negligible intrinsic, observational, and galactic effects. While searches for higher pulsar derivatives will not improve the signal sensitivity, their relative contributions can be used to learn about the frequencies present within a passing GW [66].

So far, we have assumed the pulsar timing model includes  $\ddot{P}$  (and its derivatives) such that the entire signal of ultralow-frequency GWs is fit into the timing model parameters. An alternative approach is to only incorporate parameters in the timing model fit that are expected to have significant non-GW contributions. In our context, this would correspond to fitting for  $\dot{P}$  and  $\dot{P}_b$  but not fitting for  $\ddot{P}$ . With this approach, the residuals can be used to search for GWs. In fact, theoretical projections for PTA capabilities occasionally incorporate this effect in their sensitivity estimates (see, e.g., Refs. [67,68]), even though PTA collaborations have refrained from extending their existing curves into the ultralow-frequency regime. However, our approach has a few major advantages over the conventional analysis strategy. Firstly, timing model parameters for which additional internal contributions can be independently measured [e.g., the three non-GW contributions to  $\dot{P}_{b,\text{obs}}$  in Eq. (4)] allow us to exploit our knowledge of their values to boost sensitivity, a procedure that has no direct analog in a conventional residual search. This ability to subtract known contributions will become even more critical as PTA sensitivity improves to the point where experiments will detect kinematic corrections to  $\dot{P}_{\text{obs}}$ . Secondly, our analysis can be extended to search for stochastic signals in the ultralow-frequency regime [69]. This region is difficult to study via residuals alone since the residual correlator becomes nonstationary. Finally, studying the timing model parameters offers a significant computational benefit since it does not require simultaneously analyzing the residuals for all the pulsars in the array; each timing model parameter can be determined individually, and their biases can be subsequently used to search for GWs.

*Dataset description.*—We use different sets of pulsars for the two parameters of interest. For the  $\dot{P}_b$  search, we use a set of 14 binary pulsars compiled in Ref. [70] to detect the Milky Way potential. (See Ref. [71] for a similar analysis.) These pulsars were selected as they possess well-estimated intrinsic and Shklovskii contributions to the observed parameter,  $\dot{P}_{b,\text{obs}}$  [first and second terms on the right-hand side of Eq. (4)]. We must additionally include an estimate of the contribution from the Milky Way potential [the third term on the rhs of Eq. (4)], which we calculate using the MWPotential2014 model implemented in the GALPY PYTHON package [72]. We take a 20% uncertainty on the value for every pulsar, which is roughly the order of the uncertainties on galactic fit parameters in MWPotential2014

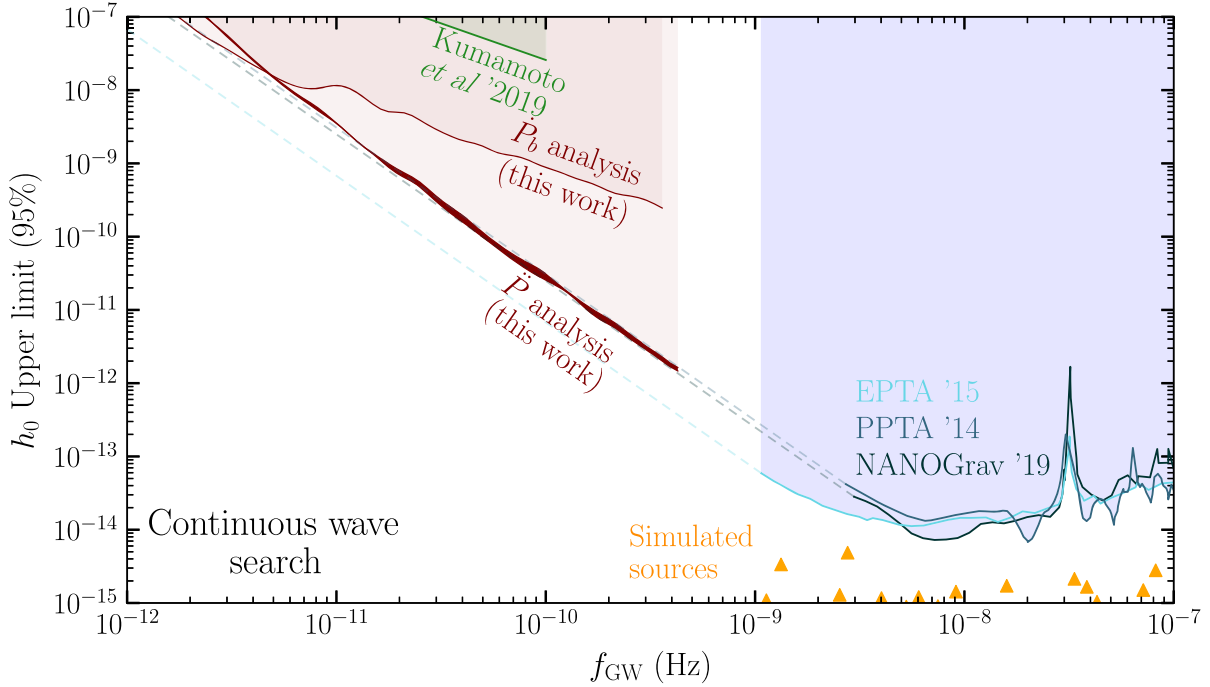


FIG. 1. Sensitivity of pulsar timing arrays to continuous-wave sources from inspirals of supermassive black hole using  $\dot{P}$  and  $\dot{P}_b$  analyses (red). For the  $\dot{P}$  analysis, we use the width of the line as an estimate of the influence of ultralow-frequency red noise (see text for details). Constraints from traditional PTA searches shown by EPTA (light blue) [73], PPTA (blue) [74], and NANOGrav (dark blue) [75]. We also show results from a previous search using statistical analysis of  $\dot{P}$  [35] (green). Finally, we plot the output from a simulation of SMBH mergers (orange) [76].

[72]. We then subtract these three contributions from  $\dot{P}_{b,\text{obs}}/P_b$ , estimating the line-of-sight acceleration  $a_{\text{GW}}$  for each pulsar. A summary of all the pulsars used in both analyses, including the size of the intrinsic, Shklovskii, and MW contributions, can be found in the SM [45].

Measurements of  $\dot{P}$  are not published by the pulsar timing collaborations for most pulsars. Instead, we use a study carried out in Ref. [58], which searched for evidence of jerk within 49 pulsars from EPTA [49] and PPTA [48] data (with additional timing data from Ref. [60]). Of the 49 pulsars, three are unsuitable for searching for ultralow-frequency GWs, and we omit these in our analysis.

The measured values of  $\dot{P}_{\text{obs}}$  provided by Ref. [58] include the effects of dispersion measure (DM) variation and red noise. DM variation was assumed to give rise to a Kolmogorov turbulence spectrum with an amplitude extracted by earlier fits performed by the pulsar timing collaborations. The red noise spectrum was modeled as a broken power law with a spectral index and amplitude. Red noise was included by adding  $A_k \sin(2\pi f_k/T) + B_k \cos(2\pi f_k/T)$  to the residuals, where  $f_k = k/T$  with  $k = 1, 2, \dots$  and  $A_k$  and  $B_k$  are randomly sampled from the power spectrum. By construction, this method only incorporates red noise above  $1/T$  and does not account for potential ultralow-frequency red noise, which influences the timing model similar to gravitational waves but is

uncorrelated among the pulsars. If left as a free parameter, the ultralow-frequency red noise contribution would eliminate any prospect for gravitational wave detection. Instead, we estimate the induced variance in the fit parameters, assuming the spectrum persists as a broken power law below  $1/T$  and using the fit parameters from EPTA [49] and PPTA [48], as described in the SM [45]. We add the square root of this variance in quadrature with the uncertainty on  $\dot{P}_{\text{obs}}$ . Because of uncertainty in these estimates, we perform a second analysis, where we inflate the value of the red noise estimate by an order of magnitude. Even with these inflated values, the effect of ultralow-frequency red noise does not appreciably alter the limits (see Fig. 1). For completeness, we also estimated the influence of ultralow-frequency red noise on  $\dot{P}_b$  with the formalism introduced in the SM [45]. We find it is always negligible with respect to the current uncertainties on  $\dot{P}_{b,\text{obs}}$ .

Given that all non-GW contributions are either already accounted for in the measured  $\dot{P}$  values (as is the case for DM and red noise) or are significantly below the current uncertainties on these values (as is the case for the intrinsic, kinematic, and Galactic contributions), we produce a set of line-of-sight jerk estimates by taking  $j_{\text{GW}} = \dot{P}_{\text{obs}}/P$  for these 46 pulsars.

Note that at this time, the published datasets we use are six to seven years outdated; our limits would be improved

by an updated analysis. Furthermore, adding existing NANOGrav data to the analysis would substantially improve the sensitivity.

*Results and discussion.*—We conduct two separate analyses using the  $a_{\text{GW}}$  and  $j_{\text{GW}}$  datasets, performing log-likelihood ratio tests for the presence of a gravitational wave signal within each dataset (see SM [45] and Ref. [77] for details). We do not find significant evidence for a continuous-wave signal using the datasets described in the previous section. Consequently, we set limits on  $h_0$  as a function of  $f_{\text{GW}}$  and find the results shown in Fig. 1 (red) for the  $\dot{P}_b$  and  $\ddot{P}$  analyses. For comparison, we also show limits for continuous-wave sources from EPTA (light blue) [73], PPTA (blue) [74], and NANOGrav (dark blue) [75], as well as previous limits set using all-sky correlations of  $\dot{P}$  [35] in green. We extend the PTA curves according to the expected scaling behavior of conventional analyses in the ultralow-frequency regime [68]; however, we note that none of the collaborations have published limits in this frequency range. To emphasize the power of exploring the ultralow-frequency regime for SMBH inspirals, we also show the results of a simulation of individual SMBH sources [76]. The low-frequency cutoff of simulated sources depends sensitively on the astrophysical assumptions about SMBH binaries at separations near 1 pc; the  $\dot{P}_b$  and  $\ddot{P}$  analyses are a novel probe into physics on these scales.

For frequencies  $10 \text{ pHz} \lesssim f_{\text{GW}} \lesssim 450 \text{ pHz}$ , we find the sensitivity

$$h_0 \simeq \begin{cases} 1.8 \times 10^{-10} \left( \frac{400 \text{ pHz}}{f_{\text{GW}}} \right) & (\dot{P}_b \text{ analysis}) \\ 1.6 \times 10^{-12} \left( \frac{400 \text{ pHz}}{f_{\text{GW}}} \right)^2 & (\ddot{P} \text{ analysis}) \end{cases}. \quad (6)$$

The scaling of the limits with frequency can be understood by observing that, in this range,  $a_{\text{GW}} \propto h_0 f_{\text{GW}}$  and  $j_{\text{GW}} \propto h_0 f_{\text{GW}}^2$ . The scaling of the  $\ddot{P}$  analysis agrees with the scaling of projections for searches using the residuals directly at ultralow frequencies when the timing model excludes  $\ddot{P}$  [67,68]. (This is to be expected since, in such an analysis, the unfit  $\ddot{P}$  signal is contained in the residuals.) The  $\ddot{P}$  analysis reaches a smaller strain for  $f_{\text{GW}} \gtrsim 3.5 \text{ pHz}$ , while the  $\dot{P}_b$  analysis reaches a smaller strain for  $f_{\text{GW}} \lesssim 3.5 \text{ pHz}$ . We note that a simultaneous observation of GWs using both  $\dot{P}_b$  and  $\ddot{P}$  would break the degeneracy of  $h_0$  and  $f_{\text{GW}}$ . As such, including both may prove a critical tool for upcoming analyses.

The behavior of the limits changes outside this frequency range. For  $f_{\text{GW}} \lesssim 10 \text{ pHz}$ , the GW frequency is below  $d_a^{-1}$  for the most sensitive pulsars such that the GW influences both the SSB and the pulsar similarly. This causes a partial cancellation between the two terms in Eq. (1). This only holds at leading order in  $f_{\text{GW}}$  such that the sensitivity in each case falls off as an additional power of frequency, i.e.,

$a_{\text{GW}} \propto h_0 d_a f_{\text{GW}}^2$  and  $j_{\text{GW}} \propto h_0 d_a f_{\text{GW}}^3$  in this regime. For frequencies near or above  $T^{-1}$ ,  $\dot{P}_b$  and  $\ddot{P}$  are not well approximated by time derivatives of  $v_{\text{GW}}$ . For this reason, we cut off our analysis at  $f_{\text{GW}} = (4T)^{-1}$  with  $T = 22$  (17.7) yr, corresponding to the longest pulsar observation time in the  $\dot{P}_b$  ( $\ddot{P}$ ) dataset.

The sensitivity achieved by searching for drifts in the timing model parameters is competitive with current PTA strategies near 1 nHz. If the gravitational wave signal observed by the pulsar timing collaborations [78–80] is from SMBH inspirals, then a corresponding signal is expected in the sub-nHz band. Consequently, correlated timing model drifts should appear in the near future and may be the key to uncovering the physics of SMBH binaries at separations near 1 pc. Such correlations may already be detectable by NANOGrav or with more current EPTA and PPTA observations, strongly motivating the case for the collaborations to perform measurements of  $\dot{P}$  with their existing data.

While the focus of our work has been on continuous-wave sources, our study can be extended to search for a stochastic ultralow-frequency GW background [69]. Apart from the signal induced by SMBH inspirals, a stochastic signal in this frequency range could also be an indication of a turbulent QCD phase transition [27,28] or a consequence of new global [26] or gauge symmetries [81]. If a stochastic background were present, it could, in principle, be distinguished from a continuous source through the different correlations in the timing model parameters. We leave the viability of discriminating continuous and stochastic sources for future work. By studying biases in the timing model parameters, we open a new frequency range for exploration for PTA analyses, with profound implications for astrophysics, cosmology, and particle physics.

We thank Sukanya Chakrabarti and Nihan Pol for useful discussions early on during this work. We also thank the anonymous referee for bringing the importance of ultralow-frequency red noise to our attention and Xiao-Jin Liu for correspondence on Ref. [58]. The research of J.D. is supported in part by NSF CAREER Grant No. PHY-1915852 and in part by the U.S. Department of Energy Grant No. DE-SC0023093. W.D. is supported in part by Department of Energy Grant No. DE-SC0010107. Part of this work was performed at the Aspen Center for Physics, which is supported by National Science Foundation Grant No. PHY-1607611.

- 
- [1] Y. Akrami *et al.* (Planck Collaboration), Planck 2018 results. X. Constraints on inflation, *Astron. Astrophys.* **641**, A10 (2020).
  - [2] Z. Arzoumanian *et al.* (NANOGrav Collaboration), The NANOGrav 12.5 yr data set: Search for an isotropic stochastic gravitational-wave background, *Astrophys. J. Lett.* **905**, L34 (2020).

- [3] B. Goncharov *et al.*, On the evidence for a common-spectrum process in the search for the nanohertz gravitational-wave background with the Parkes Pulsar Timing Array, *Astrophys. J. Lett.* **917**, L19 (2021).
- [4] S. Chen *et al.*, Common-red-signal analysis with 24-yr high-precision timing of the European Pulsar Timing Array: Inferences in the stochastic gravitational-wave background search, *Mon. Not. R. Astron. Soc.* **508**, 4970 (2021).
- [5] J. Antoniadis *et al.*, The International Pulsar Timing Array second data release: Search for an isotropic gravitational wave background, *Mon. Not. R. Astron. Soc.* **510**, 4873 (2022).
- [6] R. Abbott *et al.* (KAGRA, Virgo, LIGO Scientific Collaborations), Upper limits on the isotropic gravitational-wave background from Advanced LIGO and Advanced Virgo's third observing run, *Phys. Rev. D* **104**, 022004 (2021).
- [7] P. Amaro-Seoane *et al.*, Laser Interferometer Space Antenna, [arXiv:1702.00786](https://arxiv.org/abs/1702.00786).
- [8] M. Maggiore *et al.*, Science case for the Einstein Telescope, *J. Cosmol. Astropart. Phys.* **03** (2020) 050.
- [9] S. Dimopoulos, P.W. Graham, J.M. Hogan, M.A. Kasevich, and S. Rajendran, Gravitational wave detection with atom interferometry, *Phys. Lett. B* **678**, 37 (2009).
- [10] L. Hui, S. T. McWilliams, and I.-S. Yang, Binary systems as resonance detectors for gravitational waves, *Phys. Rev. D* **87**, 084009 (2013).
- [11] T. Dolch *et al.* (NANOGrav Collaboration), Single-source gravitational wave limits from the J1713 + 0747 24-hr global campaign, *J. Phys. Conf. Ser.* **716**, 012014 (2016).
- [12] C. J. Moore, D. P. Mihaylov, A. Lasenby, and G. Gilmore, Astrometric search method for individually resolvable gravitational wave sources with Gaia, *Phys. Rev. Lett.* **119**, 261102 (2017).
- [13] S. A. Klioner, Gaia-like astrometry and gravitational waves, *Classical Quantum Gravity* **35**, 045005 (2018).
- [14] J. Darling, A. E. Truebenbach, and J. Paine, Astrometric limits on the stochastic gravitational wave background, *Astrophys. J.* **861**, 113 (2018).
- [15] Y. Wang, K. Pardo, T.-C. Chang, and O. Doré, Gravitational wave detection with photometric surveys, *Phys. Rev. D* **103**, 084007 (2021).
- [16] M. A. Fedderke, P. W. Graham, B. Macintosh, and S. Rajendran, Astrometric gravitational-wave detection via stellar interferometry, *Phys. Rev. D* **106**, 023002 (2022).
- [17] M. A. Fedderke, P. W. Graham, and S. Rajendran, Asteroids for  $\mu\text{Hz}$  gravitational-wave detection, *Phys. Rev. D* **105**, 103018 (2022).
- [18] D. Blas and A. C. Jenkins, Bridging the  $\mu\text{Hz}$  gap in the gravitational-wave landscape with binary resonances, *Phys. Rev. Lett.* **128**, 101103 (2022).
- [19] D. Blas and A. C. Jenkins, Detecting stochastic gravitational waves with binary resonance, *Phys. Rev. D* **105**, 064021 (2022).
- [20] N. Aggarwal *et al.*, Challenges and opportunities of gravitational-wave searches at MHz to GHz frequencies, *Living Rev. Relativity* **24**, 4 (2021).
- [21] V. Domcke, C. Garcia-Cely, and N. L. Rodd, Novel search for high-frequency gravitational waves with low-mass axion haloscopes, *Phys. Rev. Lett.* **129**, 041101 (2022).
- [22] A. Berlin, D. Blas, R. Tito D'Agnolo, S. A. R. Ellis, R. Harnik, Y. Kahn, and J. Schütte-Engel, Detecting high-frequency gravitational waves with microwave cavities, *Phys. Rev. D* **105**, 116011 (2022).
- [23] M. C. Begelman, R. D. Blandford, and M. J. Rees, Massive black hole binaries in active galactic nuclei, *Nature (London)* **287**, 307 (1980).
- [24] A. Sesana, Gravitational wave emission from binary supermassive black holes, *Classical Quantum Gravity* **30**, 244009 (2013).
- [25] C. J. Moore and A. Vecchio, Ultra-low-frequency gravitational waves from cosmological and astrophysical processes, *Nat. Astron.* **5**, 1268 (2021).
- [26] C.-F. Chang and Y. Cui, Stochastic gravitational wave background from global cosmic strings, *Phys. Dark Universe* **29**, 100604 (2020).
- [27] A. Neronov, A. Roper Pol, C. Caprini, and D. Semikoz, NANOGrav signal from magnetohydrodynamic turbulence at the QCD phase transition in the early Universe, *Phys. Rev. D* **103**, L041302 (2021).
- [28] A. Brandenburg, E. Clarke, Y. He, and T. Kahniashvili, Can we observe the QCD phase transition-generated gravitational waves through pulsar timing arrays?, *Phys. Rev. D* **104**, 043513 (2021).
- [29] B. Bertotti, B. J. Carr, and M. J. Rees, Limits from the timing of pulsars on the cosmic gravitational wave background, *Mon. Not. R. Astron. Soc.* **203**, 945 (1983).
- [30] S. M. Kopeikin, Binary pulsars as detectors of ultralow frequency gravitational waves, *Phys. Rev. D* **56**, 4455 (1997).
- [31] S. M. Kopeikin, Millisecond and binary pulsars as nature's frequency standards. II. The effects of low-frequency timing noise on residuals and measured parameters, *Mon. Not. R. Astron. Soc.* **305**, 563 (1999).
- [32] V. A. Potapov, Y. P. Ilyasov, V. V. Oreshko, and A. E. Rodin, Timing results for the binary millisecond pulsar J1640 + 2224 obtained on the RT-64 radio telescope in Kalyazin, *Astron. Lett.* **29**, 241 (2003).
- [33] S. M. Kopeikin and V. A. Potapov, Millisecond and binary pulsars as nature's frequency standards. 3. Fourier analysis and spectral sensitivity of timing observations to low-frequency noise, *Mon. Not. R. Astron. Soc.* **355**, 395 (2004).
- [34] M. S. Pshirkov, Investigating ultra-long gravitational waves with measurements of pulsar rotational parameters, *Mon. Not. R. Astron. Soc.* **398**, 1932 (2009).
- [35] N. Yonemaru, H. Kumamoto, K. Takahashi, and S. Kuroyanagi, Sensitivity of new detection method for ultra-low-frequency gravitational waves with pulsar spin-down rate statistics, *Mon. Not. R. Astron. Soc.* **478**, 1670 (2018).
- [36] H. Kumamoto, Y. Imasato, N. Yonemaru, S. Kuroyanagi, and K. Takahashi, Constraints on ultra-low-frequency gravitational waves with statistics of pulsar spin-down rates, *Mon. Not. R. Astron. Soc.* **489**, 3547 (2019).
- [37] H. Kumamoto, S. Hisano, and K. Takahashi, Constraints on ultra-low-frequency gravitational waves with statistics of pulsar spin-down rates. II. Mann-Whitney U test, *Publ. Astron. Soc. Jpn.* **73**, 1001 (2021).
- [38] T. Kikunaga, S. Hisano, H. Kumamoto, and K. Takahashi, Constraints on ultra-low-frequency gravitational waves

- from an eccentric supermassive black hole binary, *Mon. Not. R. Astron. Soc.* **509**, 5188 (2021).
- [39] Alternative approaches to detect ultralow-frequency GWs are through astrometric lensing [40–42] and searching for cosmic microwave background spectral distortions [43]. While the sensitivity of these techniques is currently well below the capabilities of pulsar timing in the frequency range we consider, they form the strongest constraints for even lower frequencies.
- [40] C. R. Gwinn, T. M. Eubanks, T. Pyne, M. Birkinshaw, and D. N. Matsakis, Quasar proper motions and low frequency gravitational waves, *Astrophys. J.* **485**, 87 (1997).
- [41] L. G. Book and E. E. Flanagan, Astrometric effects of a stochastic gravitational wave background, *Phys. Rev. D* **83**, 024024 (2011).
- [42] J. Darling, A. E. Truebenbach, and J. Paine, Astrometric limits on the stochastic gravitational wave background, *Astrophys. J.* **861**, 113 (2018).
- [43] T. Kite, A. Ravenni, S. P. Patil, and J. Chluba, Bridging the gap: Spectral distortions meet gravitational waves, *Mon. Not. R. Astron. Soc.* **505**, 4396 (2021).
- [44] R. T. Edwards, G. B. Hobbs, and R. N. Manchester, TEMPO2, a new pulsar timing package. II. The timing model and precision estimates, *Mon. Not. R. Astron. Soc.* **372**, 1549 (2006).
- [45] See Supplemental Material, which includes Refs. [46–60], at <http://link.aps.org/supplemental/10.1103/PhysRevLett.132.101403> for a description of the signal, details on our analysis, cross-checks on our statistical method, estimates of the size of kinematic and galactic corrections to  $\dot{P}$ , and a discussion of ultralow-frequency red noise.
- [46] D. J. Reardon *et al.*, The parkes pulsar timing array second data release: Timing analysis, *Mon. Not. R. Astron. Soc.* **507**, 2137 (2021).
- [47] E. Fonseca *et al.*, The nanograv nine-year data set: Mass and geometric measurements of binary millisecond pulsars, *Astrophys. J.* **832**, 167 (2016).
- [48] D. J. Reardon *et al.*, Timing analysis for 20 millisecond pulsars in the Parkes Pulsar Timing Array, *Mon. Not. R. Astron. Soc.* **455**, 1751 (2015).
- [49] G. Desvignes *et al.*, High-precision timing of 42 millisecond pulsars with the European Pulsar Timing Array, *Mon. Not. R. Astron. Soc.* **458**, 3341 (2016).
- [50] E. Fonseca, I. H. Stairs, and S. E. Thorsett, A comprehensive study of relativistic gravity using PSR B1534 + 12, *Astrophys. J.* **787**, 82 (2014).
- [51] M. F. Alam *et al.*, The NANOGrav 12.5 yr data set: Wideband timing of 47 millisecond pulsars, *Astrophys. J. Suppl. Ser.* **252**, 5 (2020).
- [52] M. Kramer *et al.*, Tests of general relativity from timing the double pulsar, *Science* **314**, 97 (2006).
- [53] W. W. Zhu *et al.*, Tests of gravitational symmetries with pulsar binary J1713 + 0747, *Mon. Not. R. Astron. Soc.* **482**, 3249 (2018).
- [54] P. C. C. Freire, N. Wex, G. Esposito-Farèse, J. P. W. Verbiest, M. Bailes, B. A. Jacoby, M. Kramer, I. H. Stairs, J. Antoniadis, and G. H. Janssen, The relativistic pulsar white dwarf binary PSR J1738 + 0333 II. The most stringent test of scalar-tensor gravity, *Mon. Not. R. Astron. Soc.* **423**, 3328 (2012).
- [55] K. Liu *et al.*, A revisit of PSR J1909-3744 with 15-yr high-precision timing, *Mon. Not. R. Astron. Soc.* **499**, 2276 (2020).
- [56] I. Cognard *et al.*, A massive-born neutron star with a massive white dwarf companion, *Astrophys. J.* **844**, 128 (2017).
- [57] D. L. Kaplan *et al.*, PSR J1024-0719: A millisecond pulsar in an unusual long-period orbit, *Astrophys. J.* **826**, 86 (2016).
- [58] X. J. Liu, M. J. Keith, C. Bassa, and B. W. Stappers, Correlated timing noise and high precision pulsar timing: Measuring frequency second derivatives as an example, *Mon. Not. R. Astron. Soc.* **488**, 2190 (2019).
- [59] A. V. Bilous, T. T. Pennucci, P. Demorest, and S. M. Ransom, A broadband radio study of the average profile and giant pulses from PSRr B1821-24a, *Astrophys. J.* **803**, 83 (2015).
- [60] V. M. Kaspi, J. H. Taylor, and M. F. Ryba, High-precision timing of millisecond pulsars. III. Long-term monitoring of PSRs B1855 + 09 and B1937 + 21, *Astrophys. J.* **428**, 713 (1994).
- [61] M. Maggiore, *Gravitational Waves. Vol. 2: Astrophysics and Cosmology* (Oxford University Press, New York, 2018).
- [62] H. Wahlquist, The Doppler response to gravitational waves from a binary star source., *Gen. Relativ. Gravit.* **19**, 1101 (1987).
- [63] I. S. Shklovskii, Possible causes of the secular increase in pulsar periods, *Sov. Astron.* **13**, 562 (1970).
- [64] D. R. Lorimer and M. Kramer, *Handbook of Pulsar Astronomy* (Cambridge University Press, 2012).
- [65] X. J. Liu, C. G. Bassa, and B. W. Stappers, High-precision pulsar timing and spin frequency second derivatives, *Mon. Not. R. Astron. Soc.* **478**, 2359 (2018).
- [66] Additionally, it has been suggested in Ref. [30] that the secular drift in the projected semimajor axis ( $x$ ) of a binary pulsar could be used for ultralow-frequency GW detection. Since  $\dot{x}/x$  has a Shklovskii contribution identical to that of  $\dot{P}_b/P_b$ , measurements of GWs using both  $\dot{x}$  and  $P_b$  are highly correlated and would not substantially boost experimental sensitivity.
- [67] C. J. Moore, S. R. Taylor, and J. R. Gair, Estimating the sensitivity of pulsar timing arrays, *Classical Quantum Gravity* **32**, 055004 (2015).
- [68] J. S. Hazboun, J. D. Romano, and T. L. Smith, Realistic sensitivity curves for pulsar timing arrays, *Phys. Rev. D* **100**, 104028 (2019).
- [69] W. DeRocco and J. A. Dror, Searching for stochastic gravitational waves below a nanohertz, *Phys. Rev. D* **108**, 103011 (2023).
- [70] S. Chakrabarti, P. Chang, M. T. Lam, S. J. Vigeland, and A. C. Quillen, A measurement of the galactic plane mass density from binary pulsar accelerations, *Astrophys. J. Lett.* **907**, L26 (2021).
- [71] D. F. Phillips, A. Ravi, R. Ebadi, and R. L. Walsworth, Milky Way accelerometry via millisecond pulsar timing, *Phys. Rev. Lett.* **126**, 141103 (2021).
- [72] J. Bovy, GALPY: A PYTHON library for galactic dynamics, *Astrophys. J. Suppl. Ser.* **216**, 29 (2015).
- [73] S. Babak *et al.*, European pulsar timing array limits on continuous gravitational waves from individual supermassive black hole binaries, *Mon. Not. R. Astron. Soc.* **455**, 1665 (2015).

- [74] X.-J. Zhu *et al.*, An all-sky search for continuous gravitational waves in the Parkes Pulsar Timing Array data set, *Mon. Not. R. Astron. Soc.* **444**, 3709 (2014).
- [75] K. Aggarwal, Z. Arzoumanian, P. T. Baker *et al.*, The NANOGrav 11 yr data set: Limits on gravitational waves from individual supermassive black hole binaries, *Astrophys. J.* **880**, 116 (2019).
- [76] B. Kocsis and A. Sesana, Gas driven massive black hole binaries: Signatures in the nHz gravitational wave background, *Mon. Not. R. Astron. Soc.* **411**, 1467 (2011).
- [77] S. Algeri, J. Aalbers, K. D. Morå, and J. Conrad, Searching for new phenomena with profile likelihood ratio tests, *Nat. Rev. Phys.* **2**, 245 (2020).
- [78] G. Agazie *et al.* (NANOGrav Collaboration), The NANOGrav 15 yr data set: Evidence for a gravitational-wave background, *Astrophys. J. Lett.* **951**, L8 (2023).
- [79] J. Antoniadis *et al.* (EPTA Collaboration), The second data release from the European Pulsar Timing Array III. Search for gravitational wave signals, *Astron. Astrophys.* **678**, A50 (2023).
- [80] D. J. Reardon *et al.*, Search for an isotropic gravitational-wave background with the Parkes pulsar timing Array, *Astrophys. J. Lett.* **951**, L6 (2023).
- [81] N. Kitajima and K. Nakayama, Dark photon dark matter from cosmic strings and gravitational wave background, *J. High Energy Phys.* **08** (2023) 068.